

The effect of the electron-phonon interaction of the conductivity of impure metals

M. Yu. Reizer and A. V. Sergeev

V. I. Lenin State Teaching Institute, Moscow

(Submitted 3 November 1986)

Zh. Eksp. Teor. Fiz. **92**, 2291–2304 (June 1987)

We have investigated corrections to the impurity conductivity originating from interference between the electron-phonon and electron-impurity interactions. The conductivity was calculated both by a method based on the quantum kinetic equation and by the linear response method. We show that because of peculiarities in the screening of transverse electromagnetic fields in metals, the interference corrections to the impurity conductivity from longitudinal and transverse phonons have differing signs. However, since the longitudinal sound velocity is larger than the transverse sound velocity, the total correction turns out to be negative, leading to an increase in resistance with temperature. We also consider the interference of electron-magnon and electron-impurity interactions in ferromagnetic metals.

INTRODUCTION

Recently, the problem of how electron scattering affects and is affected by the kinetic properties of normal metals has attracted considerable interest. At sufficiently low temperatures the conductivity of "dirty" metals is determined by localization and electron-electron interaction effects¹; however, as the temperature increases, the processes considered in this paper, which are related to interference between electron-phonon and electron-impurity interactions, become significant.

The influence of these processes on the resistivity of normal metals was investigated in Refs. 2–4. A quasiclassical kinetic equation was used in Ref. 2, which did not permit consideration of all the various quantum interference effects. In fact, the only processes discussed in this paper involve inelastic scattering of electrons by impurities.⁽¹⁾ In Ref. 3, the linear response method was used, which makes it possible to include all these interference processes. However, the authors of Ref. 3 arrived at the erroneous conclusion that only inelastic electron-impurity scattering processes were important, in agreement with Ref. 2. In Ref. 4, a temperature-dependent correction to the impurity resistivity was found by using the quantum kinetic equation in the same form as in Refs. 2 and 3; however, this correction is due to impurity renormalization of the vertex which describes the interaction of an electron with longitudinal phonons. For $q_T l \gg l$ ($q_T = T/u$, u is the sound velocity, l is the mean free path of electrons due to impurity scattering), the corrections to the resistivity found in Refs. 2–4 have the form

$$\Delta\rho_{e-ph-imp}/\rho_0 \sim T^2/\varepsilon_F p_F u > 0 \quad (1)$$

which gives rise to an increase in the resistivity with temperature (ε_F and p_F are the Fermi energy and momentum, and ρ_0 is the residual resistivity).

However, in fact that situation turns out to be more complex than this. As we show in this paper, there are additional processes due to electron-phonon-impurity interference, which lead to corrections to the resistivity similar to (1); however, they are of opposite sign. In the region of attainable temperatures $T > (u/c)(\varepsilon_F p_F u)^{1/2}$ (c is the velocity of light), these processes are found to be significant only for longitudinal phonons, while interactions with transverse phonons are "exhausted" by inelastic electron-impurity

scattering processes. This latter assertion is based on an analysis of the screening of longitudinal and transverse electromagnetic fields presented in Section 2. As a result, the corrections to the resistivity due to the interactions of electrons with longitudinal and transverse phonons have different signs. However, since the longitudinal velocity u_l is larger than the transverse velocity u_t , the sum of these two corrections to the resistivity turns out to be positive.

The basic results of the paper are obtained in Section 3, using the quantum kinetic equation. In Section 4 we briefly discuss the linear response method. In the kinetic equation method we analyze a comparatively small number of diagrams; however, in calculating the contributions from these diagrams it is necessary to include a different kind of correction for each diagram. The linear response method allows us to calculate the contributions from each diagram in the same way; however, the number of diagrams which must be investigated is considerably increased. In our opinion,⁵ kinetic phenomena related to electron-phonon-impurity interference are most conveniently discussed in a comoving coordinate system (CCS), i.e., a reference frame in which the lattice is at rest. This method of calculating $\Delta\rho_{e-ph-imp}$ is briefly described in Section 5. In Section 6, the method developed above is applied to the investigation of interference between electron-magnon and electron-impurity interactions in a ferromagnetic metal. In the conclusion, we analyze the results so obtained and discuss the experimental situation.

2. EFFECTIVE VERTICES FOR LONGITUDINAL AND TRANSVERSE PHONONS

In Keldysh's diagram technique,⁶ the Green's functions for electrons and phonons, and also the electron and phonon self-energies, are represented by the matrices

$$\hat{G} = \begin{pmatrix} 0 & G^A \\ G^R & G^c \end{pmatrix}, \quad \hat{D} = \begin{pmatrix} 0 & D^A \\ D^R & D^c \end{pmatrix},$$

$$\hat{\Sigma} = \begin{pmatrix} \Sigma^c & \Sigma^R \\ \Sigma^A & 0 \end{pmatrix}, \quad \hat{\Pi} = \begin{pmatrix} \Pi^c & \Pi^R \\ \Pi^A & 0 \end{pmatrix}. \quad (2)$$

In the absence of the electron-phonon interaction, the electron Green's function averaged over impurity positions equals

$$G_0^R(\mathbf{p}, \varepsilon) = [G_0^A(\mathbf{p}, \varepsilon)]^* = (\varepsilon - \xi_{\mathbf{p}} + i/2\tau)^{-1},$$

$$\xi_{\mathbf{p}} = (p^2 - p_F^2)/2m. \quad (3)$$

Here, τ is the electron's momentum relaxation time due to impurity scattering, and m is the electron mass.

To linear order in the electric field, G^C takes the form⁴:

$$G^C(\mathbf{p}, \varepsilon) = S(\mathbf{p}, \varepsilon) [G^A(\mathbf{p}, \varepsilon) - G^R(\mathbf{p}, \varepsilon)]$$

$$+ {}^{1/2}i \{S(\mathbf{p}, \varepsilon), G^A(\mathbf{p}, \varepsilon) + G^R(\mathbf{p}, \varepsilon)\}, \quad (4)$$

where the last term denotes a Poisson bracket. In the case of a constant electric field,

$$\{A, B\} = e\mathbf{E} \left(\frac{\partial A}{\partial \varepsilon} \frac{\partial B}{\partial \mathbf{p}} - \frac{\partial A}{\partial \mathbf{p}} \frac{\partial B}{\partial \varepsilon} \right). \quad (5)$$

In this section we limit ourselves to calculating the equilibrium vertex, i.e., we will assume that the distribution function $S(\mathbf{p}, \varepsilon) = S_0(\varepsilon) = -\tanh(\varepsilon/2T)$. The corrections to the equilibrium function and to the Poisson bracket which are proportional to the electric field will be taken into account in the following section.

Elastic scattering of electrons by impurities is expressed by the matrix $|V_{e-imp}|(\sigma_x)_{ij}$, where σ_x is the familiar Pauli matrix. The impurity potential we will assume to be short-range and isotropic:

$$1/\tau = \pi v N_{imp} |V_{e-imp}|^2, \quad v = mp_F/\pi^2, \quad (6)$$

where N_{imp} is the impurity concentration.

Following Ref. 7, we will treat the electron-phonon interaction as an interaction of electrons and ions with an electromagnetic field; this allows us to discuss both transverse and longitudinal phonons in the same way. In contrast to Ref. 7, our goal is to construct an effective electron-phonon interaction vertex, which is necessary to calculate the self-energy of an electron.

The interaction of electrons with an electromagnetic field is described by the Hamiltonian

$$H_{e-photon} = - \sum_{\mathbf{p}} \sum_{\mathbf{q}}' \varphi_{\mathbf{q}} c_{\mathbf{p}+\mathbf{q},s}^+ c_{\mathbf{p},s} + \sum_{\mathbf{p}} \sum_{\mathbf{q}} \frac{2\mathbf{p}-\mathbf{q}}{2mc} \mathbf{A}_{\mathbf{q}} c_{\mathbf{p}+\mathbf{q},s}^+ c_{\mathbf{p},s}$$

$$+ \sum_{\mathbf{p}} \sum_{\mathbf{q},\mathbf{q}'} \frac{1}{2mc^2} \mathbf{A}_{\mathbf{q}} \mathbf{A}_{\mathbf{q}'} c_{\mathbf{p}+\mathbf{q}+\mathbf{q}',s}^+ c_{\mathbf{p},s}, \quad (7)$$

where $\varphi_{\mathbf{q}}$, $\mathbf{A}_{\mathbf{q}}$ are Fourier components of the scalar and vector potentials; $c_{\mathbf{p},s}^+$ is a creation operator for an electron with momentum \mathbf{p} and spin s ; the prime on the summation sign indicates that terms with $q = 0$ are omitted.

The Hamiltonian (7) corresponds to the following electron-phonon interaction vertices:

$$a^0 = -1, \quad a^1 = \mathbf{p}/mc, \quad a^{11} = 1/2mc^2, \quad (8)$$

assuming that $q \ll p$. From here on, the index 0 will refer to vertices describing interactions with scalar potentials, while 1 will denote interactions with vector potentials.

The Hamiltonians for interactions of ions and impurities with the electromagnetic field have the form

$$H_{ion-photon} = \int d\mathbf{r} \left[\rho_{ion}(\mathbf{r}) \varphi(\mathbf{r}) - \frac{1}{c} \mathbf{j}_{ion}(\mathbf{r}) \mathbf{A}(\mathbf{r}) \right], \quad (9)$$

$$H_{imp-photon} = \int d\mathbf{r} \left[\rho_{imp}(\mathbf{r}) \varphi(\mathbf{r}) - \frac{1}{c} \mathbf{j}_{imp}(\mathbf{r}) \mathbf{A}(\mathbf{r}) \right], \quad (10)$$

where the charge density and current are given by the equations

$$\rho_{ion}(\mathbf{r}) = Z_{ion} \sum_{\alpha} \delta(\mathbf{r} - \mathbf{R}_{\alpha}),$$

$$\rho_{imp} = (Z_{imp} - Z_{ion}) \sum_{\beta} \delta(\mathbf{r} - \mathbf{R}_{\beta}), \quad (11)$$

$$\mathbf{j}_{ion}(\mathbf{r}) = \frac{Z_{ion}}{M} \sum_{\alpha} \mathbf{P}_{\alpha} \delta(\mathbf{r} - \mathbf{R}_{\alpha}),$$

$$\mathbf{j}_{imp} = \left(\frac{Z_{imp}}{M_{imp}} - \frac{Z_{ion}}{M} \right) \sum_{\beta} \mathbf{P}_{\beta} \delta(\mathbf{r} - \mathbf{R}_{\beta}). \quad (12)$$

Here, Z_{ion} is the valence of atoms in the host lattice and Z_{imp} is the impurity valence; M and M_{imp} are the host and impurity masses, \mathbf{R}_{α} and \mathbf{R}_{β} their coordinates; and $\mathbf{P}_{\alpha} = M\dot{\mathbf{R}}_{\alpha}$, $\mathbf{P}_{\beta} = M_{imp}\dot{\mathbf{R}}_{\beta}$. The absolute value of the electron charge is included in the definition of the electromagnetic potentials.

Let us first investigate the Hamiltonian $H_{ion-photon}$. We extract from it terms which are linear in the displacement of the ions from their equilibrium positions $\Delta\mathbf{R}_{\alpha} = \mathbf{R}_{\alpha} - \mathbf{R}_{\alpha 0}$ ($\mathbf{R}_{\alpha 0}$ is the equilibrium position of an ion). We then express $\Delta\mathbf{R}_{\alpha}$ and $\dot{\Delta}\mathbf{R}_{\alpha}$ in terms of creation and annihilation operators for phonons $b_{\mathbf{q}\lambda}^+$, $b_{\mathbf{q}\lambda}$ (λ is the index of a phonon branch):

$$\Delta\mathbf{R} = \sum_{\mathbf{q}\lambda} \frac{\mathbf{e}_{\lambda} e^{i\mathbf{q}\mathbf{r}}}{(2MN\omega_{\mathbf{q}\lambda})^{1/2}} (b_{\mathbf{q}\lambda} + b_{-\mathbf{q}\lambda}^+), \quad (13)$$

$$\dot{\Delta}\mathbf{R} = -i \sum_{\mathbf{q}\lambda} \frac{\mathbf{e}_{\lambda} \omega_{\mathbf{q}\lambda} e^{i\mathbf{q}\mathbf{r}}}{(2MN\omega_{\mathbf{q}\lambda})^{1/2}} (b_{\mathbf{q}\lambda} - b_{-\mathbf{q}\lambda}^+). \quad (14)$$

As a result, we obtain the phonon-photon interaction Hamiltonian

$$H_{phon-photon} = \sum_{\mathbf{q}\lambda} (Q_{\mathbf{q}\lambda}^0 \Phi_{\mathbf{q}\lambda}^0 \varphi_{\mathbf{q}} + Q_{\mathbf{q}\lambda}^1 \Phi_{\mathbf{q}\lambda}^1 \mathbf{A}_{\mathbf{q}}), \quad (15)$$

where the vertices Q are shown in Fig. 1, and equal

$$Q_{\mathbf{q}\lambda}^0 = i \frac{ZN\mathbf{q}\mathbf{e}_{\lambda}}{(2MN\omega_{\mathbf{q}\lambda})^{1/2}}, \quad Q_{\mathbf{q}\lambda}^1 = -i \frac{ZN\omega_{\mathbf{q}\lambda}\mathbf{e}_{\lambda}}{c(2MN\omega_{\mathbf{q}\lambda})^{1/2}}, \quad (16)$$

$$\Phi_{\mathbf{q}\lambda}^0 = b_{\mathbf{q}\lambda} + b_{-\mathbf{q}\lambda}^+, \quad \Phi_{\mathbf{q}\lambda}^1 = b_{\mathbf{q}\lambda} - b_{-\mathbf{q}\lambda}^+, \quad (17)$$

where N is the number of unit cells, and $\omega_{\mathbf{q}\lambda}$ is the phonon frequency; $\omega_{\mathbf{q}\lambda} = u_{\lambda} q$, where u_{λ} is the sound velocity; and \mathbf{e}_{λ} is the polarization vector. Under conditions of charge neutrality the relation

$$Z_{ion} N_{ion} + Z_{imp} N_{imp} = n_e = ZN$$

holds, where n_e is the electron density.

In order to include the two kinds of operators Φ^0 and

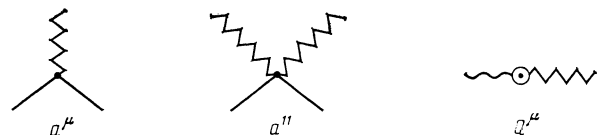


FIG. 1. Electron-photon interaction vertices, a^{μ} , a^{11} ; Q^{μ} is the phonon-photon interaction vertex.

Φ^1 , we introduce the matrix Green's function for phonons:

$$D_{\mu\nu}(\mathbf{q}, \lambda, t) = -i \langle T_t (\tilde{\Phi}_{q\lambda}^\nu(t) \tilde{\Phi}_{q\lambda}^\mu(0)) \rangle, \quad \nu, \mu = 0, 1, \quad (18)$$

where $\tilde{\Phi}_{q\lambda}^\nu(t)$ is an operator in the Heisenberg representation and T_t is the symbol for time-ordering. As will be shown below, we will require only the function $D_{00}(\mathbf{q}, \omega)$ in what follows, which we will write without the lower indices:

$$D^R(\mathbf{q}, \omega) = [D^A(\mathbf{q}, \omega)]^* = (\omega - \omega_q + i0)^{-1} - (\omega + \omega_q + i0)^{-1}. \quad (19)$$

The phonons are assumed to be in equilibrium; hence,

$$D^C(\mathbf{q}, \omega) = (2N_\omega + 1) [D^R(\mathbf{q}, \omega) - D^A(\mathbf{q}, \omega)],$$

$$N_\omega = (e^{\omega/T} - 1)^{-1}. \quad (20)$$

The Green's function for the electromagnetic potentials also are in matrix form $V_{\mu\nu}$. In the Coulomb gauge, $\text{div } \mathbf{A} = 0$; the matrix $V_{\mu\nu}$ is diagonal in the momentum representation, and when screening is included takes the form^{7,8}

$$V_{00}^R(\mathbf{q}, \omega) = 4\pi e^2 / [q^2 - 4\pi e^2 P_{00}^R(\mathbf{q}, \omega)]. \quad (21)$$

$$[V_{11}^R(\mathbf{q}, \omega)]_{mn} = V_{11}^R(\mathbf{q}, \omega) T_{mn},$$

$$V_{11}^R(\mathbf{q}, \omega) = \frac{4\pi e^2 c^2}{\omega^2 - c^2 q^2 - 4\pi e^2 c^2 P_{11}^R(\mathbf{q}, \omega)}, \quad (22)$$

m, n denote the Cartesian coordinates x, y, z ; if the vector \mathbf{q} lies along the z -axis, then

$$T_{mn} = \delta_{mn} - q_m q_n / q^2 = \begin{bmatrix} 1 & 0 & 0 \\ 0 & 1 & 0 \\ 0 & 0 & 0 \end{bmatrix}; \quad (23)$$

$P_{\mu\mu}^R(\mathbf{q}, \omega)$ is the polarization operator (Fig. 2) with the vertices a_x^μ [corresponding to (8), $a_x^1 = p_x / mc$; for the scalar vertex a^0 we define $a_x^0 = a^0 = -1$]. In calculations using the Keldysh technique, the vertices must be multiplied by the tensor K_{ij}^k (the upper index for bosons, the lower for electrons):

$$K_{ij}^1 = 2^{-1/2} \delta_{ij}, \quad K_{ij}^2 = 2^{-1/2} (\sigma_x)_{ij}. \quad (24)$$

Then

$$P_{\mu\mu}^R(\mathbf{q}, \omega) = \frac{n_e}{m c^2} \delta_{\mu 1}$$

$$- 2i \int \frac{d\mathbf{p} d\varepsilon}{(2\pi)^4} (a_x^\mu)^2 K_{ij}^1 [G_0(\mathbf{p}, \varepsilon)]_{ki} [G_0(\mathbf{p} + \mathbf{q}, \varepsilon + \omega)]_{jl} K_{kl}^2. \quad (25)$$

For $ql \gg l$ we have

$$P_{00}^R(\mathbf{q}, \omega) = -\nu, \quad P_{11}^R(\mathbf{q}, \omega) = -i\pi\nu\omega v_F / 4qc^2. \quad (26)$$

For normal metals, the condition for strong screening

$$V_{\mu\nu} = \text{zigzag} = \text{zigzag} + \text{zigzag} \text{ with loop},$$

$$P_{\mu\mu} = \text{loop} = a_x^\mu \text{ loop} a_x^\mu + a_x^\mu \text{ loop} a_x^\mu,$$

FIG. 2. Equation for the Green's function of the electromagnetic field: the thin zigzag ("sawtoothed") line denotes the bare interaction, while $P_{\mu\mu}$ denotes the polarization operator.

of longitudinal fields is satisfied:

$$|(4\pi e^2 / q^2) P_{00}^R(\mathbf{q}, \omega)| \gg 1 \quad (27)$$

and thus

$$V_{00}^R = -(P_{00}^R)^{-1} = \nu^{-1}.$$

For the transverse fields, the applicability of the strong-screening condition

$$|4\pi e^2 c^2 (\omega^2 - c^2 q^2)^{-1} P_{11}^R(\mathbf{q}, \omega)| \gg 1 \quad (28)$$

depends on the values of ω and q . For the frequencies and wave vectors of the phonons of interest to us, i.e., $\omega \sim T$, $q \sim q_T = T/u$, the inequality (28) is found to hold only in the extreme low-temperature regime:

$$T \ll T_1 = (u/c) (u p_F \kappa / 3m)^{1/2}, \quad \kappa^2 = 4\pi e^2 \nu. \quad (29)$$

For practically attainable temperatures, the transverse electromagnetic fields are not screened, i.e., $V_{11}^R = -4\pi e^2 / q^2$.

The effective electron-phonon interaction vertex is shown in Fig. 3:

$$(g^\mu)_{ij}^k = a^\mu V_{\mu\mu} Q^\mu K_{ij}^k, \quad \mu = 0, 1. \quad (30)$$

Using (8) and (27), we find

$$(g^0)_{ij}^k = i g_{q\lambda} K_{ij}^k, \quad g_{q\lambda} = {}^2/3 \varepsilon_F (2MN\omega_{q\lambda})^{-1/2} q e_\lambda. \quad (31)$$

From the condition for weak screening of the transverse electromagnetic field we have for thermal phonons

$$g^1 / g^0 \sim (T_1 / T)^2 \ll 1. \quad (32)$$

Condition (32) justifies the assertion made earlier that it is necessary to include only the function $D_{00}(\mathbf{q}, \omega)$ in calculations. As a result, for $T > T_1$, the Hamiltonian $H_{\text{ion-phot}}$ leads to an interaction of the electrons only with longitudinal phonons.

In an analogous fashion, we can also discuss the Hamiltonian $H_{\text{imp-phot}}$ (10). Taking into account the shift of the impurities from their equilibrium positions, we obtain an effective vertex γ which describes inelastic scattering of electrons by the impurities. Since the momentum transferred by the electron in this process is of order p_F while the frequency ω is of order T , according to the analysis given above of the screening of the electromagnetic field, the term $\mathbf{j}_{\text{imp}} \mathbf{A}$ in the Hamiltonian (10) can be neglected. Including only the sca-

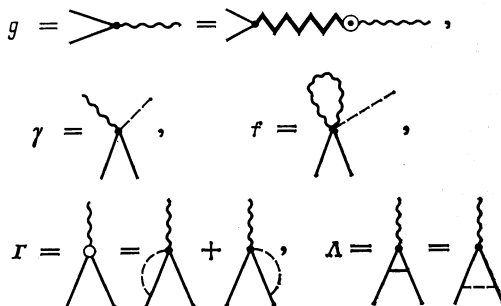


FIG. 3. Vertices g, γ describing electron-phonon scattering and inelastic scattering of electrons by impurities; f, Γ, Δ are effective vertices.

lar potential interaction, we have⁵

$$\gamma_{ij}^k = i |V_{e-imp}| (2MN\omega_{q\lambda})^{-1/2} (\mathbf{p}-\mathbf{p}') \mathbf{e}_\lambda K_{ij}^k. \quad (33)$$

In order to calculate the conductivity, we also need a vertex which describes inelastic scattering of electrons by impurities through interactions with two phonons, which we immediately write in the effective form (see Fig. 3):

$$f_{ij} = - \frac{\{(\mathbf{p}-\mathbf{p}') \mathbf{e}_\lambda\}^2}{4MN\omega_{q\lambda}} |V_{e-imp}| \int \frac{d\mathbf{q} d\omega}{(2\pi)^4} D^c(\mathbf{q}, \omega) \frac{1}{2} (\sigma_x)_{ij}. \quad (34)$$

The factor 1/2 appears when we go to Keldysh's triangular representation.⁶

Let us introduce the effective vertex Γ shown in Fig. 3:

$$\begin{aligned} \Gamma_{22}^1 &= -\Gamma_{11}^1 = \Gamma, & \Gamma_{11}^2 &= [S_0(\varepsilon) - S_0(\varepsilon + \omega)] \Gamma, \\ \Gamma_{12}^1 &= S_0(\varepsilon) \Gamma, & \Gamma_{12}^2 &= \Gamma_{21}^2 = \Gamma_{22}^2 = 0, \\ \Gamma_{21}^1 &= -S_0(\varepsilon + \omega) \Gamma, & \Gamma &= \mathbf{p} \mathbf{e}_\lambda / 2\tau (MN\omega_{q\lambda})^{1/2}. \end{aligned} \quad (35)$$

Along with Γ , we also construct the vertex Λ for longitudinal phonons (Fig. 3), which takes into account electron-phonon-impurity interference to lowest order in perturbation theory; for $ql \gg 1$:

$$\begin{aligned} \Lambda_{22}^1 &= \Lambda, & \Lambda_{11}^2 &= [S_0(\varepsilon + \omega) - S_0(\varepsilon)] \Lambda, \\ \Lambda_{12}^1 &= S_0(\varepsilon) \Lambda, & \Lambda_{11}^1 &= [1 - 2S_0(\varepsilon)S_0(\varepsilon + \omega)] \Lambda, \\ \Lambda_{21}^1 &= -S_0(\varepsilon + \omega) \Lambda, & \Lambda_{12}^2 &= \Lambda_{21}^2 = \Lambda_{22}^2 = 0, \\ \Lambda &= i\pi g_{q\lambda} / 2^{1/2} ql. \end{aligned} \quad (36)$$

Thus, the interaction of electrons with longitudinal phonons is described by the vertices g , γ , f , Γ , and Λ ; for thermal transverse phonons we need only include γ , f .

3. THE KINETIC-EQUATION METHOD

In calculating the temperature-dependent corrections to the impurity conductivity $\Delta\sigma(T)$, we will use a method based on the quantum kinetic equation developed in Ref. 4. When linearized in the external electric field, the kinetic equation for the electron distribution function $S(\mathbf{p}, \varepsilon)$ can be represented in the form

$$e\mathbf{v}\mathbf{E}\partial S_0(\varepsilon)/\partial\varepsilon = I_{e-imp}(S) + I_{e-ph}(S) + I_{e-ph-imp}(S), \quad (37)$$

where the collision integrals on the right side include electron-impurity and electron-phonon scattering along with interference between them. Each collision integral is related to a corresponding self-energy part by the relations

$$I(S) = I_0(S) + \delta I(S), \quad I_0 = -i[\Sigma^c - S(\Sigma^A - \Sigma^R)], \quad (38)$$

$$\delta I = -i[\delta\Sigma^c - S_0(\delta\Sigma^A - \delta\Sigma^R)] + 1/2\{\Sigma^A + \Sigma^R, S\}. \quad (39)$$

In Eqs. (37)–(39) we have dropped the arguments $(\varepsilon, \mathbf{p})$; in what follows we will omit these arguments for brevity in the collision integrals, self-energy parts and distribution functions. The $\delta\Sigma$ terms are corrections to (5) in Poisson-bracket form; they are linear in electric field, and appear when the diagram technique is used to describe nonequilibrium processes in the momentum representation. When the basic momentum relaxation mechanism is scattering by impurities, the kinetic equation (37) can be solved by iteration, using $S = S_0 + \varphi_0 + \varphi_1$. Without including phonons, the nonequilibrium correction to the distribution takes the well-

known form:

$$\varphi_0(\mathbf{p}, \varepsilon) = -e\tau\mathbf{v}\mathbf{E}\partial S_0(\varepsilon)/\partial\varepsilon. \quad (40)$$

To first order in perturbation theory we have

$$\begin{aligned} \varphi_1(\mathbf{p}, \varepsilon) &= [I_{e-ph}(S_0 + \varphi_0) + I_{e-ph-imp}(S_0 + \varphi_0) \\ &\quad + \delta_{ph} I_{e-imp}(S_0 + \varphi_0)] \tau. \end{aligned} \quad (41)$$

The last term in (41) is due to phonon renormalization of the electron density of states in the electron-impurity collision integral, i.e., this integral is not calculated with the zero-order Green's function (3) but rather includes the phonon correction

$$\delta_{ph} G^A(S) = (G_0^A)^2 [\Sigma_{e-ph}^A(S) + \Sigma_{e-ph-imp}^A(S)]. \quad (42)$$

The electric current is determined by the expression

$$\mathbf{j} = \sigma\mathbf{E} = 2e \int \frac{d\mathbf{p} d\varepsilon}{(2\pi)^4} \mathbf{v} S(\mathbf{p}, \varepsilon) \text{Im} G^A(\mathbf{p}, \varepsilon), \quad (43)$$

from which it is clear that the source of the temperature-dependent correction $\Delta\sigma$ is both the phonon correction to the distribution function (41) and the correction to $\text{Im} G^A$:

$$\begin{aligned} \delta_{ph} \mathbf{j} &= \Delta\sigma(T)\mathbf{E} = 2e \int \frac{d\mathbf{p} d\varepsilon}{(2\pi)^4} \mathbf{v} \{ \varphi_1 \text{Im} G_0^A + \varphi_0 \text{Im} [\delta_{ph} G^A(S_0)] \\ &\quad + S_0 \text{Im} [\delta_{ph} G^A(\varphi_0)] + S_0 \text{Im} \delta G^A(S_0) \}, \end{aligned} \quad (44)$$

where δG^A is the correction due to the Poisson bracket:

$$\delta G^A(S) = (G_0^A)^2 [\delta\Sigma_{e-ph}^A(S) + \delta\Sigma_{e-ph-imp}^A(S)]. \quad (45)$$

The electron self-energy diagrams related to electron-impurity and electron-phonon interactions are shown in Figs. 4.1, and 4.2. The next diagrams (Figs. 4.3–4.7) are interference diagrams. Under the conditions $ql \gg 1$, $p_F l \gg 1$, these diagrams take into account the electron-phonon interaction to first order in perturbation theory, while the electron-impurity interaction is taken into account since the electron Green's function is chosen in the form (3); in calculating the vertex renormalization due to impurities, we need work only to first order in the electron-impurity interaction.

Turning to calculation of the contributions from each of the diagrams, we will first make some comments. The calculations show that for any diagram, the second term in (44) is cancelled by that part of $\varphi_1 \text{Im} G_0^A$ which is related to the electron-impurity collision integral [the last term in (41)]. Furthermore, in the integral over ε in (44), only the following combinations of distribution functions are nonnegative:

$$f\left(\frac{\omega}{T}\right) = \frac{1}{2} \int S_0(\varepsilon + \omega) \frac{\partial S_0(\varepsilon)}{\partial\varepsilon} d\varepsilon = \frac{\partial}{\partial\omega} \left(\frac{\omega}{2T} \text{cth} \frac{\omega}{2T} \right), \quad (46)$$

$$\frac{1}{2} \int (2N_\omega + 1) \frac{\partial S_0(\varepsilon)}{\partial\varepsilon} d\varepsilon = -\text{cth} \frac{\omega}{2T}, \quad (47)$$

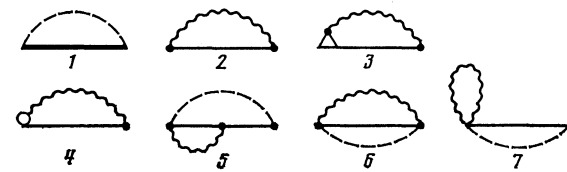


FIG. 4. Self-energy diagrams for electrons in the laboratory system. Graphs 3–5 and 7 actually denote two diagrams each: the one shown in the figure and another one which differs from it by an interchange of vertices.

along with the terms symmetric to them under interchange of $S_0(\varepsilon)$ and $S_0(\varepsilon + \omega)$; the first of these terms (46) depends on the electron temperature, while the second depends on phonon temperature. Finally, as is clear from (42) and (45), all corrections to $\text{Im } G^A(\mathbf{p}, \varepsilon)$ in (44) contain the factor

$$\frac{1}{\pi\nu\tau} \int \frac{d\mathbf{p}}{(2\pi)^3} [G_0^A(\mathbf{p}, \varepsilon)]^2 G_0^R(\mathbf{p}+\mathbf{q}, \varepsilon+\omega) \left(\frac{\mathbf{p}\mathbf{q}}{pq}\right)^n \ll \frac{1}{(ql)^2},$$

$$n=0, 1,$$

which must be retained only when calculating the contribution from $\Sigma_{\text{e-ph}}$. The interference diagrams contain an additional small factor $(ql)^{-1}$ from the vertices, γ , Γ and Λ ; therefore, the corrections from them to $\text{Im } G^A(\mathbf{p}, \varepsilon)$ are not included.

Let us first discuss the longitudinal phonons. The diagram $\Sigma_{\text{e-ph}}$ (Fig. 5.2) gives both the well-known Bloch correction to the impurity conductivity and corrections of the form (1). The first arises because of the usual collision integral of electrons with phonons $I_0(\mathbf{p}, \varepsilon)$ (38):

$$I_0(\mathbf{p}, \varepsilon) = - \int \frac{d\mathbf{q} d\omega}{(2\pi)^4} 8g_{q_i}^2 \text{Im } G_0^A(\mathbf{p}+\mathbf{q}, \varepsilon+\omega) \times \text{Im } D^R(\mathbf{q}, \omega) R(\varepsilon, \omega), \quad (48)$$

where

$$R(\varepsilon, \omega) = \frac{1}{4} \{ (2N_0 + 1) [S(\varepsilon) - S(\varepsilon + \omega)] + S(\varepsilon)S(\varepsilon + \omega) - 1 \}.$$

Using the collision integral so obtained, let us determine the correction to the distribution function $\varphi_1(p, \varepsilon)$ (41), which should be substituted into (44) to calculate the conductivity. As a result, we find

$$\Delta\sigma_{\text{e-ph}}/\sigma_0 = -60\pi\xi(5)\beta_i\tau T^5/(p_F u_i)^4, \quad (49)$$

where

$$\beta_i = (2/3\varepsilon_F)^2 \nu / 2MNu_i^2, \quad \xi(5) \approx 1.03, \quad \sigma_0 = 1/3 e^2 \nu v_F^2 \tau.$$

Expression (49) was obtained earlier in Ref. 4, and in contrast with the pure-metal case is derived under the assumption that the basic mechanism for electron momentum relaxation is scattering by impurities, i.e., under conditions appropriate to a "weak" Matthiessen's rule.⁹

For the corrections to the conductivity of the form (1) from the diagrams in 4.2, the remaining part of the collision integral δI is found to be important; $\delta\Sigma$ appears only because of δG^c [the last term in (4)]:

$$\delta I = \text{Im} \int \frac{d\mathbf{q} d\omega}{(2\pi)^4} e \text{Ev} g_{q_i}^2 S_0(\varepsilon + \omega) \times \frac{\partial S_0(\varepsilon)}{\partial \varepsilon} [G_0^A(\mathbf{p}+\mathbf{q}, \varepsilon + \omega)]^2 D^A(\mathbf{q}, \omega). \quad (50)$$

The correction to the conductivity on δI is calculated using (41), (44). The third term in (44), caused by the correction $\delta_{\text{ph}} G^A$ due to the nonequilibrium $\Sigma_{\text{e-ph}}^A$ (42), gives exactly the same contribution to $\Delta\sigma(T)$. The final correction to the conductivity connected with diagram 4.2, equals

$$\Delta\sigma_2(T)/\sigma_0 = 1/8 \pi^2 \beta_i T^2 / \varepsilon_F p_F u_i. \quad (51)$$

The interference diagrams 4.3–4.6 give only corrections to the conductivity in the form (1). Let us note that the effective vertices Λ and Γ , which enter into the diagrams 4.3

and 4.4, themselves depend on the electron distribution function. The equilibrium vertices were determined from Eqs. (35), (36), while the nonequilibrium corrections to them are obtained by taking $\varphi_0(\mathbf{p}, \varepsilon)$ into account, and equal

$$\begin{aligned} \delta_\varphi \Lambda_{12}^i &= -\delta_\varphi \Gamma_{12}^i = \frac{\partial S_0(\varepsilon)}{\partial \varepsilon} \psi(\mathbf{q}, \lambda), \\ \delta_\varphi \Lambda_{21}^i &= -\delta_\varphi \Gamma_{21}^i = -\frac{\partial S_0(\varepsilon + \omega)}{\partial \varepsilon} \psi(\mathbf{q}, \lambda), \\ \delta_\varphi \Lambda_{11}^2 &= -\delta_\varphi \Gamma_{11}^2 = \left[\frac{\partial S_0(\varepsilon + \omega)}{\partial \varepsilon} - \frac{\partial S_0(\varepsilon)}{\partial \varepsilon} \right] \psi(\mathbf{q}, \lambda), \\ \psi(\mathbf{q}, \lambda) &= \varepsilon_F \mathbf{E} \mathbf{e}_\lambda / 3(MN\omega_{q\lambda})^{1/2}. \end{aligned} \quad (52)$$

There are no corrections to the vertices with other indices. Since the diagram Σ_3 (Fig. 4.3) has the same index structure as Σ_4 , while it is clear from Eq. (52) that the vertices $\sigma_\varphi \Gamma$ and $\delta_\varphi \Lambda$ are opposite in sign, the contributions from diagrams Σ_3 and Σ_4 calculated using the nonequilibrium vertices (52) cancel each other. The collision integral including only the equilibrium vertices for diagram 4.3 equals

$$I_0(\mathbf{p}, \varepsilon) = -2 \text{Re} \int \frac{d\mathbf{q} d\omega}{(2\pi)^4} e \tau \nu \mathbf{E} g_{q_i} \Lambda S_0(\varepsilon + \omega) \times \frac{\partial S_0(\varepsilon)}{\partial \varepsilon} G_0^A(\mathbf{p}+\mathbf{q}, \varepsilon + \omega) D^A(\mathbf{q}, \omega). \quad (53)$$

Correspondingly, for diagram 4.4 we have

$$I_0(\mathbf{p}, \varepsilon) = 2 \text{Im} \int \frac{d\mathbf{q} d\omega}{(2\pi)^4} e \tau \nu \mathbf{E} g_{q_i} \Gamma S_0(\varepsilon + \omega) \times \frac{\partial S_0(\varepsilon)}{\partial \varepsilon} G_0^A(\mathbf{p}+\mathbf{q}, \varepsilon + \omega) D^A(\mathbf{q}, \omega). \quad (54)$$

Substituting the expressions for the collision integrals (53), (54) into (44), and taking into account (41), we obtain

$$\Delta\sigma_3(T) = \Delta\sigma_4(T) = \left(\frac{1}{\pi^2} - \frac{1}{12} \right) \frac{\pi^4 \beta_i T^2}{2\varepsilon_F p_F u_i} \sigma_0. \quad (55)$$

We calculate corrections to the conductivity related to the fifth, sixth, and seventh diagrams in an analogous way. Let us note that for each of the diagrams 4.2 to 4.5 individually and for the sum of the diagrams 4.6 and 4.7, contributions from the combinations of distribution functions (47) cancel each other. In addition, the fifth and sixth diagrams give contributions containing the combination of distribution functions (46) which also cancel:

$$\Delta\sigma_5(T) = -\Delta\sigma_6(T) = \frac{2}{3} \frac{\pi^2 \beta_i T^2}{\varepsilon_F p_F u_i} \sigma_0. \quad (56)$$

Calculations show that in the case of transverse phonons, the contributions from the sixth and seventh diagrams equal the corresponding contributions for longitudinal phonons when u_i is replaced by u_\perp . Hence, the total correction to the conductivity connected with interference between electron-phonon and electron-impurity interactions for one longitudinal and two transverse branches equals

$$\frac{\Delta\sigma_{\text{e-ph-imp}}}{\sigma_0} = \left[\frac{4}{3\pi^2} - \frac{1}{12} - \frac{8}{3\pi^2} \left(\frac{u_\perp}{u_i} \right)^3 \right] \frac{\pi^4 \beta_i T^2}{2\varepsilon_F p_F u_i}. \quad (57)$$

From (57) it is clear that the sign $\Delta\sigma_{\text{e-ph-imp}}$ for longitudinal phonons is positive, while for transverse phonons it is negative.

tive. The total result depends on the ratio of sound velocities u_l/u_t . We also point out the fact that $\Delta\sigma_{e-ph-imp}$ depends only on the electron temperature, while $\Delta\sigma_{e-ph}$ depends on both the electron and phonon temperatures.

4. THE LINEAR RESPONSE METHOD

In the linear response method, the correction to the impurity conductivity is determined by the equation

$$\Delta\sigma = e^2 \lim_{\Omega \rightarrow 0} \Pi^R(\Omega) / (-i\Omega), \quad (58)$$

where $\Pi^R(\Omega)$ is the retarded loop with two vector vertices

$$B_{ij}^k = (Ev/E) K_{ij}^k. \quad (59)$$

As was already noted in the Introduction, for calculations involving the same order of perturbation theory, it is necessary to analyze a considerably larger number of diagrams in the linear response method than with the kinetic-equation method. Therefore, in Fig. 5 we limit ourselves to depicting only the important diagrams. The function $\Pi^R(T)$ is encountered only in the case where Π^R contains the products G_0^C and $G_0^C D^C$. It can be shown that in the first case only the combinations $G_0^C(\epsilon)G_0^C(\epsilon + \omega + \Omega)$ and $G_0^C(\epsilon + \Omega)G_0^C(\epsilon + \omega)$ give a nonzero contribution to the conductivity. For each of the diagrams 5.1–5.8, the contributions from all possible orderings of the indices leading to the combination $G_0^C D^C$ mutually cancel. Analogous contributions from diagrams 5.9–5.12 cancel only in the total sum. The final result for the correction to the conductivity coincides with that calculated in Section 3 by the kinetic-equation method. In this case, the second diagram in Fig. 4 corresponds to diagrams 5.1–5.3, the sixth and the seventh diagrams to diagrams 5.9–5.12. Diagrams 5.4 and 5.6 are comparable to the third and the fourth diagrams in Fig. 4, calculated by the kinetic-equation method with equilibrium vertices. Diagrams 5.5, 5.7, and 5.8 in linear response theory correspond to inclusion of the nonequilibrium vertices in diagrams 4.3 and 4.4, along with diagram 4.5.

5. THE COMOVING COORDINATE SYSTEM

As we mentioned before, use of a CCS to describe the electron-phonon interaction allows us to ignore inelastic

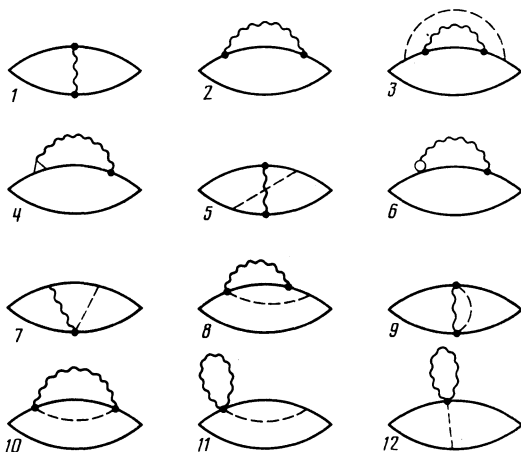


FIG. 5. Diagrams which contribute to the conductivity in the linear-response method. For asymmetric graphs only one diagram is shown.

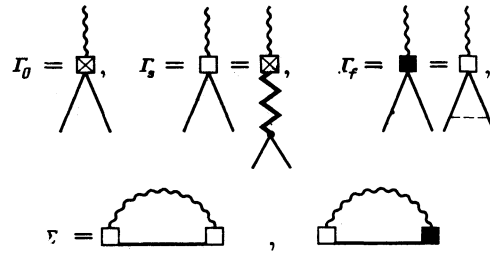


FIG. 6. Vertices which describe the electron-phonon interaction and the self-energy diagrams of electrons in the CCS.

scattering of electrons by impurities, which significantly simplifies the calculation.

The bare electron-phonon interaction vertex in a CCS equals^{5,10,11}

$$(\Gamma_0)_{ij}^k = -i \frac{(\mathbf{pq})(\mathbf{pe}_\lambda)}{m(2MN\omega_{q\lambda})^{1/2}} K_{ij}^k. \quad (60)$$

For longitudinal phonons, inclusion of screening effects leads to the vertex

$$(\Gamma_s)_{ij}^k = i(1-3x^2)g_{ij}^k, \quad x = \mathbf{pq}/pq, \quad (61)$$

where the vertex g_{ij}^k is defined in (31). For transverse phonons, the weak screening implies that the vertex Γ_s retains the form (60).

Renormalization of the vertex Γ_s due to impurities leads to the vertex Γ_f shown in Fig. 6. In the case of longitudinal phonons the vertex $(\Gamma_f)_{ij}^k$ calculated with equilibrium distribution functions coincides with the vertex Λ_{ij}^k (36), and the nonequilibrium correction satisfies $\delta_\varphi \Gamma_f = 0$. For transverse phonons, on the other hand, the equilibrium vertex satisfies $\Gamma_f = 0$ while the nonequilibrium vertex satisfies $\delta_\varphi (\Gamma_f)_{ij}^k = -\delta_\varphi \Lambda_{ij}^k$, where $\delta_\varphi \Lambda$ is defined by (52).

In solving this problem by the kinetic-equation method, we encounter the self-energy diagrams shown in Fig. 6. Corrections to the self-energy from these diagrams are calculated in a way analogous to the corrections from the diagrams in Figs. 4.2 and 4.3 discussed in Section 3. Let us simply exhibit the final results for the interference contributions from the diagrams of Figs. 6.1, 6.2:

$$\Delta\sigma_1 = \left[\frac{4}{3\pi^2} - \frac{2}{\pi^2} \left(\frac{u_l}{u_t} \right)^3 \right] \frac{\pi^4 \beta_l T^2}{2\varepsilon_F p_F u_l} \sigma_0, \quad (62)$$

$$\Delta\sigma_2 = - \left[\frac{1}{12} + \frac{2}{3\pi^2} \left(\frac{u_l}{u_t} \right)^3 \right] \frac{\pi^4 \beta_l T^2}{2\varepsilon_F p_F u_l} \sigma_0. \quad (63)$$

The total correction, as we could have anticipated, coincides with expression (57).

6. IMPURE FERROMAGNETIC METALS

The approach used in this paper can be applied to finding interference corrections to the impurity resistivity of a metal due to interactions of electrons with any Bose excitations. Let us discuss, for example, the impure ferromagnetic metal. The interaction of electrons with magnons we will describe by the s - d exchange Hamiltonian.¹² When we include only the one-magnon processes

$$H_{s-d} = -J \left(\frac{2S}{N} \right)^{1/2} \sum_{\mathbf{q}, \mathbf{p}} (a_{\mathbf{q}} c_{\mathbf{p}+\mathbf{q}}^+ c_{\mathbf{p}} + a_{\mathbf{q}}^+ c_{\mathbf{p}}^+ c_{\mathbf{p}+\mathbf{q}}), \quad (64)$$

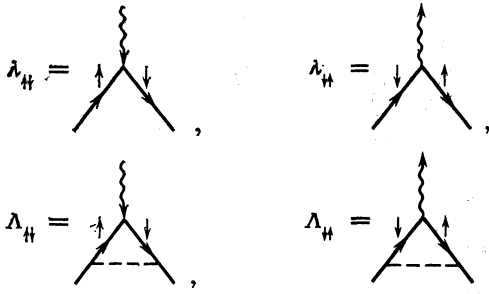


FIG. 7. Vertices for the electron-magnon interaction.

where a_q^+ is a magnon creation operator, J is the exchange integral, and N is the number of magnetic atoms with spin S . The magnon Green's function and magnon spectrum have the form

$$D^R(q, \omega) = (\omega - \omega_q + i0)^{-1}, \quad \omega_q = Aq^2, \quad A = \Theta_c / p_F^2, \quad (65)$$

where $\Theta_c = aJ^2 / \varepsilon_F$ ($a \sim 1$) is the Curie temperature.

The spectrum of electrons for each of the spin-split subbands is given by the equation $\varepsilon_{\tau, \pm} = (p^2 / 2m) \mp JS$, while the vertex $\lambda_{\tau, \pm}$ related to magnon absorption and the vertex $\lambda_{\tau, \pm}$ related to magnon emission according to (64) satisfy $\lambda_{\tau, \pm} = \lambda_{\tau, \pm} = -J(2S/N)^{1/2}$.

Following Section 2, we introduce the effective vertices $(\Lambda_{\tau, \pm})_{ij}^k$ and $(\Lambda_{\tau, \pm})_{ij}^k$ (Fig. 7), which take into account electron-magnon impurity interference to lowest order. The vertices $(\Lambda_{\tau, \pm})_{ij}^k$ and $(\Lambda_{\tau, \pm})_{ij}^k$, calculated by including the equilibrium distribution functions, are analogous to the vertex Λ_{ij}^k in (36), and can be obtained from (36) by substituting $\Lambda \equiv \Lambda_{22}^1$ for $\Lambda_{\tau, \pm}$ and $\Lambda_{\tau, \pm}$ respectively, where

$$\Lambda_{\tau, \pm} = -(\Lambda_{\tau, \pm})^* = -J \left(\frac{S}{N} \right)^{1/2} \frac{i}{2ql} \ln \frac{ql + \omega\tau + 2JS\tau + i}{-ql + \omega\tau + 2JS\tau + i}. \quad (66)$$

When the conditions $q_T \gg q_0 = 2JS / v_F$, $q_T l \gg 1$, $Aq_T^2 = T$ are fulfilled, the subband splitting can be neglected and

$$\Lambda_{\tau, \pm} = \Lambda_{\tau, \pm} = -J \left(\frac{S}{N} \right)^{1/2} \frac{\pi}{2ql}. \quad (67)$$

Then corrections to the impurity conductivity due to electron-magnon-impurity interference can be obtained if in the diagrams shown in Figs. 4.2, 4.3, or in Figs. 5.1–5.5, which contain the vertex $g_{q\tau}$, we substitute for the latter the quantity $J(2S/N)^{1/2}$ and take into account (65). Finally we obtain

$$\frac{\Delta\sigma_{e-m}}{\sigma_0} = -\frac{\pi^3 S \tau T^2 Z}{4a\Theta_c}, \quad (68)$$

$$\frac{\Delta\sigma_{e-m-imp}}{\sigma_0} = -2.5 \frac{3\pi^2}{32} S Z \left(\frac{J}{\varepsilon_F} \right)^2 \left(\frac{T}{\Theta_c} \right)^{1/2}. \quad (69)$$

In the opposite case, where $q_T \ll q_0$, $2JS\tau \gg 1$, we have

$$\Lambda_{\tau, \pm} = (\Lambda_{\tau, \pm})^* = i(S/N)^{1/2} / 2S\tau, \quad (70)$$

while the nonequilibrium corrections to the vertices satisfy $\delta_\varphi \Lambda_{\tau, \pm} = \delta_\varphi \Lambda_{\tau, \pm} = 0$.

Including diagrams like those in Figs. 4.2 and 4.3 for each subband, and adding the results, we obtain

$$\Delta\sigma_{e-m-imp} / \sigma_0 = \frac{3Z}{4S} \Gamma \left(\frac{3}{2} \right) \zeta \left(\frac{3}{2} \right) (T/\Theta_c)^{1/2}. \quad (71)$$

Let us note that $\Delta\sigma_{e-m-imp}$ from (69) and (71), just as for $\Delta\sigma_{e-ph-imp}$ from (57), contains functions only of the electron temperature. Equations like (69), (71) but containing a dependence on the magnon temperature were obtained in Ref. 13. An important difference between our results and theirs is the positive sign of the correction (71) to the conductivity $\Delta\sigma_{e-m-imp}$ for $q_T \ll q_0$, which leads to a minimum in the resistivity.

The reason for the disagreement can be found in the fact that in Ref. 13 what is calculated is not the correction to the impurity resistance but rather the imaginary part of the electron self-energy, which is artificially supplemented by a "transport factor." This approach makes it impossible in principle to include any effects of quantum interference in the resistivity.

7. CONCLUSION

The overall features of the low-temperature behavior of the resistivity of an impure metal are determined by electron-electron interaction processes,¹ and also the electron-phonon-impurity interference processes discussed in the present paper, along with the inelastic electron-phonon processes. According to the results of Sections 3–5, when we include the corrections $\Delta\sigma/\sigma_0 = -\Delta\rho/\rho_0$, the impurity resistivity due to electron-phonon-impurity interference $\Delta\rho_{e-ph-imp}$ is determined by Eq. (57); the contribution due to the longitudinal phonons has a negative sign, while the one due to transverse phonons is positive. Keeping in mind that the longitudinal velocity of sound is larger than the transverse $u_l > u_t$,¹⁴ we find that the total correction $\Delta\rho_{e-ph-imp}$ turns out to be positive, resulting in an increase of the resistivity with temperature.

In Fig. 8 we show the temperature dependence of the resistivity of an impure conductor, where $\Delta\rho_{e-ph}$ and $\Delta\rho_{e-ph-imp}$ are calculated using Eqs. (49) and (57) along with the expression from Ref. 1 for $\Delta\rho_{ee}$, i.e.,

$$\Delta\rho_{ee}/\rho_0 = -2.5(6T\tau)^{1/2} / 16(\varepsilon_F\tau)^2. \quad (72)$$

As is clear from Fig. 8, the resistivity first decreases due to $\Delta\rho_{ee}$, and then increases because of $\Delta\rho_{e-ph-imp}$ and $\Delta\rho_{e-ph}$. The correction $\Delta\rho_{e-ph-imp}$, which is quadratic in temperature, turns out to be appreciable over a wide temperature range, which makes possible its detection in experiments.

Turning to a discussion of the temperature dependence of the resistivity of impure ferromagnetic metals, we note

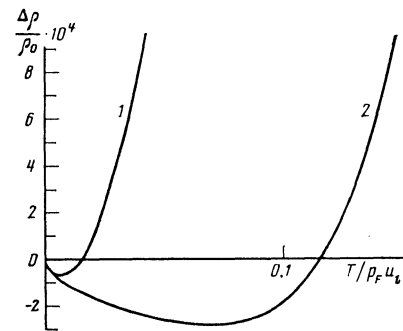


FIG. 8. Temperature dependence of the resistivity for the following parameter values: $\varepsilon_F\tau = 10$, $\varepsilon_F/p_F u_s = 100$, $\beta = 1$. For comparison, curve 2 is drawn without including $\Delta\rho_{e-ph-imp}$.

that for the characteristic value $J \sim 0.1 \varepsilon_F$ the condition $q_T = q_0$ is fulfilled at a temperature $T_0 \approx 10$ K, while the inequality $q_T l \gg 1$ is valid when the impurity concentration is not too high. In the low-temperature region $T < T_0$, the resistivity is determined by the magnitudes of $\Delta\rho_{ee}$, $\Delta\rho_{e-m-imp}$, and $\Delta\rho_{e-ph-imp}$; the first two of these are negative and give rise to the resistivity minimum. For $T > T_0$, the resistivity grows at first due to $\Delta\rho_{e-m-imp}$ and $\Delta\rho_{e-ph-imp}$, and then due to $\Delta\rho_{e-m}$ and $\Delta\rho_{e-ph}$. In low-dimensional systems the quantity $\Delta\rho_{ee}$ becomes appreciable¹ and for $T < T_0$ the relation $\Delta\rho_{ee} \gg \Delta\rho_{e-m-imp}$ holds. Actually, in recent experiments¹⁵ on thin films of iron the resistivity minimum was determined entirely by electron-electron interaction effects.

In conclusion, we note that in order to identify experimentally the corrections discussed in this paper to the resistivity of an impure metal, it is necessary to investigate not only the temperature behavior of the resistivity but also to measure the dependence on the electron mean free path.

The authors express their deepest gratitude to B. L. Al'tshuler for useful discussions, and M. E. Gershenson and Yu. V. Sharvin for clarifying the experimental situation.

⁽¹⁾We will not concern ourselves here with effects connected with distortion of the phonon spectrum due to impurities, which were also discussed in Ref. 2.

¹B. L. Altshuler and A. G. Aronov, *Electron-Electron Interactions in Disordered Systems*. Eds. A. L. Efros and M. Pollak (North-Holland: Amsterdam, Oxford, N. Y., Tokyo, 1985), p. 1.

²Yu. Kagan and A. P. Zhernov, *Zh. Eksp. Teor. Fiz.* **50**, 1107 (1966) [*Sov. Phys. JETP* **23**, 737 (1966)].

³V. N. Fleurov, P. S. Kondratenko, and A. N. Kozlov, *J. Phys. F* **10**, 1953 (1980).

⁴B. L. Al'tshuler, *Zh. Eksp. Teor. Fiz.* **75**, 1330 (1978) [*Sov. Phys. JETP* **48**, 670 (1978)].

⁵M. Yu. Reizer and A. V. Sergeev, *Zh. Eksp. Teor. Fiz.* **90**, 1056 (1986) [*Sov. Phys. JETP* **63**, 616 (1986)].

⁶L. V. Keldysh, *Zh. Eksp. Teor. Fiz.* **47**, 1515 (1964) [*Sov. Phys. JETP* **20**, 1018 (1964)].

⁷G. Grunevald and K. Scharnberg, *Z. Phys.* **B20**, 61 (1975).

⁸A. A. Abrikosov, L. P. Gor'kov, and I. E. Dzyaloshinskii, *Metody Kvantovoi Teorii Polya v Staticheskoi Fizike* (Methods of Quantum Field Theory in Statistical Physics, Prentice-Hall, Englewood Cliffs, NJ, 1963), Fizmatgiz, Moscow (1962).

⁹I. M. Lifshitz, M. Ya. Azbel', and M. I. Kaganov, *Elektronnaya Teoriya Metallov* (Electronic Theory of Metals, Consultants Bureau, New York, 1973), Nauka, Moscow (1971), p. 208.

¹⁰T. Tsuneto, *Phys. Rev.* **121**, 402 (1961).

¹¹A. Schmid, *Z. Phys.* **259**, 421 (1973).

¹²S. V. Vonsovskii, *Magnetizm* (Magnetism), Nauka, Moscow (1971).

¹³V. S. Lutovinov, O. E. Molodykh, and M. A. Savchenko, *Fiz. Met. Metalloved* **61**, 707 (1965).

¹⁴L. D. Landau and E. M. Lifshitz, *Teoriya Uprugosti* (Theory of Elasticity, 2nd Ed., Pergamon, Oxford, 1970), Nauka, Moscow (1965).

¹⁵W. W. Fuller, M. Rubinstein, S. A. Wolf, and G. A. Prins, *Proc. Intl. Conf. on Localization, Interaction and Transport Phenomena in Impure Metals*, Braunschweig, 1984 (Supplement), p. 135.

Translated by F. J. Crowne